Ultraviolet–circular dichroism spectroscopy and potentiometric study of the interaction between human serum albumin and sodium perfluorooctanoate

ARTICLE *in* BIOPOLYMERS · DECEMBER 2005

Impact Factor: 2.39 · DOI: 10.1002/bip.20353 · Source: PubMed

6 AUTHORS, INCLUDING:

Paula V Messina
Universidad Nacional del Sur
75 PUBLICATIONS **634** CITATIONS
SEE PROFILE

Xerardo Prieto
University of Santiago de Compostela
111 PUBLICATIONS **1,677** CITATIONS
SEE PROFILE

Veronica I Dodero
Bielefeld University
26 PUBLICATIONS **174** CITATIONS
SEE PROFILE

Juan M. Ruso
University of Santiago de Compostela
163 PUBLICATIONS **2,042** CITATIONS
SEE PROFILE

Paula Messina[1]
Gerardo Prieto[2]
Verónica Dodero[3]
Juan M. Ruso[1]
Pablo Schulz[1]
Félix Sarmiento[2]

[1] *Grupo de Ciencia de Superficies y Coloides, Departamento de Química, Universidad Nacional del Sur, 8000 Bahía Blanca, Argentina*

[2] *Grupo de Biofísica e Interfases, Departamento de Física Aplicada, Facultad de Física, Universidad de Santiago de Compostela, 15782 Santiago de Compostela, Spain*

[3] *Departamento de Química Orgánica, Facultad de Química, Universidad de Santiago de Compostela, 15782 Santiago de Compostela, Spain*

Ultraviolet–Circular Dichroism Spectroscopy and Potentiometric Study of the Interaction Between Human Serum Albumin and Sodium Perfluorooctanoate

Received 13 June 2005; revised 9 August 2005; accepted 9 August 2005
Published online 19 August 2005 in Wiley InterScience (www.interscience.wiley.com). DOI 10.1002/bip.20353

Abstract: *The interaction of a fluorinated surfactant, sodium perfluorooctanoate, with human serum albumin (HSA) has been investigated by a combination of ultraviolet–circular dichroism (UV-CD) spectroscopy and potentiometry (by a home-built ion-selective electrode) techniques to detect and characterize the conformational transitions of HSA. By using difference spectroscopy, the transition was followed as a function of temperature, and the data were analyzed to obtain the parameters characterizing the thermodynamics of unfolding. The results indicate that the presence of surfactant drastically changes the melting unfolding, acting as a structure stabilizer and delaying the unfolding process. Potentiometric measurements were used to determine the binding isotherms and binding capacity for this system. The isotherm shows a high affinity of surfactant molecules for HSA. The average number of surfactant*

Correspondence to: Gerardo Prieto; e-mail: faxera@usc.es
Contract grant sponsor: Spanish Ministry of Science and Technology (SMST) European Regional Development Fund (ERDF), and Xunta de Galicia (XG)
Contract grant number: MAT2002-00608 (SMST) and PGIDIT03PXI20615PN (XG)

*molecules absorbed per protein molecule (at 28 m*M *of surfactant concentration) was found to be ≈900, about 6 g of surfactant per gram of protein. The shape of the binding capacity curve and the relation between binding capacity and extend of cooperativity were examined. From these analysis, the values of* g *(number of ligand-binding sites),* K_H *(Hill binding constant), and* n_H *(Hill coefficient) were determined.* © 2005 Wiley Periodicals, Inc. Biopoly 79: 300–309, 2005

This article was originally published online as an accepted preprint. The "Published Online" date corresponds to the preprint version. You can request a copy of the preprint by emailing the Biopolymers editorial office at biopolymers@wiley.com

Keywords: *fluorinated surfactant; sodium perfluorooctanoate; human serum albumin; ultraviolet; circular dichroism; potentiometry; conformational transitions*

INTRODUCTION

The specific properties of fluorocarbons—exceptional chemical and biological inertness, high gas-dissolving capacity, low surface tension, excellent spreading characteristics, and high fluidity—have trigged numerous applications of these compounds in oxygen delivery.[1–3] Fluorinated lipids and fluorinated surfactants can be used to elaborate and stabilize various colloidal systems, including different types of emulsions, vesicles, and tubules.[4–10]

Fluorinated molecules are protein stabilizers.[11] The hydrophobic and oleophobic character of the fluorinated surfactants influences the interaction with proteins. This comportment will be reflected in the phase behavior, in the self-organization of the components, and in the stability of the different phases.

The interaction between surfactants and globular proteins have been extensively studied and reviewed.[12,13] It is well established that surfactants bind to globular proteins at concentrations below the critical micelle concentration (cmc) by a combination of ionic and hydrophobic interactions, which lead to protein–surfactants complexes.

The marginal stability of the native globular conformation of proteins, which is a delicate balance of various interactions in the proteins, is affected by the pH, temperature, and addition of small molecules such as substrates, coenzymes, inhibitors, and activators that bind especially to the native state. Studies on the interaction of surfactants with globular proteins can contributed towards an understanding of the action of surfactants as denaturants and as solubilizing agents for membranes of proteins and lipids.

Human serum albumin (HSA), a major protein component of blood plasma, is the physiological carrier for a broad range of insoluble endogenous compounds like fatty acids, lysolecithin, bilirubin, and bile salts.[14,15] It also binds to a wide variety of drugs.[16–18] This fact makes the study of interactions between a new compound with biological activity and HSA important.

In previous works[19,20] we studied the interplay between HSA and sodium perfluooctanoate ($C_7F_{15}COO^-Na^+$) at dilute and at concentrated solutions by a recently developed method based on dynamic surface tension measurements, Axysimmetric drop shape analysis (ADSA) combined with some other methods, such as the ultraviolet-visible (UV-vis) spectrophotometric technique and electrophoretic mobility measurements. Our results suggested that, at dilute surfactant solutions, protein molecules tend to locate themselves at the aqueous–air interface as well as the $C_7F_{15}COO^-Na^+$ molecules. In these conditions, proteins and surfactants molecules in the bulk solution were negligible and interactions happened only at the interface. $C_7F_{15}COO^-Na^+$ induced conformational changes on HSA molecules at the air–aqueous interface. However, at concentrated surfactant solutions, we could appreciate that $C_7F_{15}COO^-Na^+$ induces conformational changes on HSA molecules at the bulk solution and this affects the protein adsorption at the air–aqueous interphase.

To clarify still open questions, we present in this work a systematic physicochemical investigation of the water–HSA–$C_7F_{15}COO^-Na^+$ system, at 25°C.

The role of fluorinated surfactant in the supramolecular organization of proteins and protein–surfactant complexes is considered. The interactions between the components have a pronounced effect on the physicochemical properties of the above system, as well as on the structure of adducts and complexes. That is why different experimental methods were used to investigated and clarify the observed behavior.

EXPERIMENTAL

Materials

Sodium perfluorooctanoate, $C_7F_{15}COO^-Na^+$, was from Lancaster MTM Research Chemicals Ltd. and was of analytical grade (97%), product no. 16988.

HSA (albumin $\geq$ 96%, essentially fatty acid free) was purchased from Sigma Chemical Co, product no. A-1887. It has a molecular weight of 66,500 Da and contains 585 amino acid residues.

Preparation of Solutions

Sodium perfluorooctanoate ($C_7F_{15}COO^-Na^+$) and HSA stock solution (1 mg/mL) were prepared by directly dissolving the appropriate amount of surfactant and protein in ultrapure water. Both solutions were kept in a refrigerator and diluted as required.

HSA solutions were prepared without a buffer addition. The presence of buffer should affect the surface tension measurements. On other hand for a 5–8 pH range, HSA has no variation in its three structural domains (I, II, and III).[21]

Apparatus and Methods

Potentiometric determinations were made with a millivoltmeter and a CRISON pH meter. The millivoltmeter was used with an $C_7F_{15}COO^-$-ion-selective electrode, against a saturated calomel electrode.

The $C_7F_{15}COO^-$ electrode was made by gluing at one extreme of a poly(vinyl chloride) (PVC) tube a membrane made with 300 mg PVC dissolved in 50 mL tetrahydrofuran (THF) and 0.2 mL dibutylphtalate (plasticizer) and 0.167 g $Ba^{2+}(C_7F_{15}COO^-)_2$. This salt was made by mixing the appropriate amounts of $Ba(OH)_2$ and $C_7F_{15}COO^-Na^+$ aqueous solution. The insoluble $Ba^{2+}(C_7F_{15}COO^-)_2$ salt was filtered and washed several times with double-distilled water and then left to dry. The crystals were powdered and suspended in the PVC solution. Then, the suspension was left in a Petri dish to let the THF evaporate, and the resulting membrane was cut and glued to the tube. The tube was filled with an aqueous solution of 0.01 mol dm^{-3} $C_7F_{15}COO^-Na^+$ and 0.1 mol dm^{-3} KCl containing a small amount of solid AgCl. An Ag/AgCl electrode made with a silver wire was placed into the tube and connected to the millivoltmeter by a copper wire passing through a rubber plug.

The scheme of the electrode is

Ag/AgCl/reference solution/PVC membrane/sample/AgCl/Ag

The time response of the electrode depends on $C_7F_{15}COO^-Na^+$ concentrations, added electrolyte, stirring, and conditioning. In dilute solutions, the time required to get stable emf values was 10 min.

The ion-selective electrodes are sensitive to the respective free (nonaggregated) ion activity. Because we worked with diluted solution below $C_7F_{15}COO^-Na^+$ cmc, we assumed that all surfactant present in solution was free and that activities can be approach to concentrations. Then the electromotive force (emf) values, obtained to apply the ion-selective electrode over $C_7F_{15}COO^-Na^+$ aqueous solution in a (0.1–28 m*M*) concentration range, were plotted vs. logarithm of the total $C_7F_{15}COO^-Na^+$ concentration. This calibration curve was employed to obtain the $[C_7F_{15}COO^-]_{free}$ and ν values for the HSA–surfactant interaction.

Protein concentration (18 μM) remains constant during the whole experience and surfactant solution was added to vary its concentration from 0.1 to 28 m*M*.

Surfactant kinetic adsorption on HSA was followed using the same ion-selective electrode. Protein (18 μM) and surfactant (28 m*M*) were added together at the beginning of the experience and the emf values were registered in a (10–9420 segs) time range.

All experiments were performed at (25 $\pm$ 0.01) °C (sample temperature was maintained by a thermostat bath with recycling water throughout all the experiments).

Far-UV circular dichroism (CD) spectra were obtained using a JASCO-715 automatic recording spectropolarimeter (Japan) with a JASCO PTC-343 Peltier-type thermostated cell holder. Quartz cuvettes with 0.2-cm pathlength was used. CD spectra of pure HSA and HSA–$C_7F_{15}COO^-Na^+$ dilute solutions were recorded from 195 to 380 nm. Protein concentration was 8 μM and surfactant concentrations varied from 4.20 to 8.50 m*M*. The following setting were used: resolution, 1 nm; bandwidth, 1 nm; sensitivity, 50 mdeg; response time, 8 s; accumulation, 3; and scan rate 50 nm/min. Corresponding absorbance contributions of buffer solution and water were subtracted with the same instrumental parameters. Data are reported as molar ellipticity and determined as

$$[\theta]_\lambda = \frac{\theta_\lambda M_r}{ncl}$$

where c is the protein concentration, l is the path length of the cell, $[\theta]_\lambda$ is the measured ellipticity at a wavelength λ, M_r is the molecular mass of the protein, and n is the number of residues.

Temperature denaturation was followed by the CD responses at 222 nm from 5 to 80°C at a scanning rate of 1°C/min; bandwidth, 1 nm; sensitivity, 50 mdeg; and response time, 8 s.

RESULTS AND DISCUSSION

Interaction of proteins with surfactants has been a subject of extensive study for over 50 years. As pointed out by Goddard,[22,23] the studies on protein–surfactant interactions have actually laid the ground work for the current activities in the polymer–surfactant area. In this regard, proteins are essentially amphoteric polyelectrolytes, proteins exhibit secondary and tertiary structures, and this makes this inter-

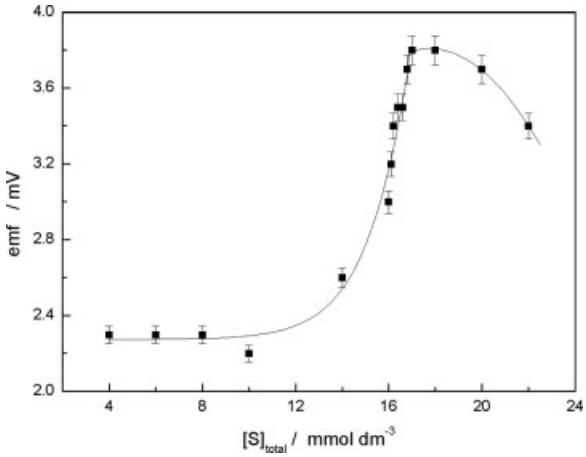

FIGURE 1 Variation of emf values vs. total surfactant concentration of sodium perfluorooctanoate ($C_7F_{15}COO^-Na^+$), $[S]_{total}$ at 25°C. The solid line is a guide to the eye.

action with surfactants much more complex. These interactions, often referred to as "surfactant binding," can lead the unfolding of proteins and sometimes their denaturation.

Most studies in the past of binding of surfactants to proteins have used the dialysis technique.[24–26] In this work, we use an ion-selective electrode to determine the amount of surfactant bound to HSA.

The interaction between HSA and $C_7F_{15}COO^-Na^+$ were inferred from the change in slope of emf values[26,27] (Figure 1).

According to emf findings, the interaction between HSA and $C_7F_{15}COO^-Na^+$ gives a true conformational change on protein molecules.

In fact, the surfactant ion activity remains nearly constant until a certain concentration is reached, $[S]_{total} = 12$ mM, where binding on HSA commences. Then there is a great intensify of emf that corresponds to the HSA–surfactant union.

At low surfactant concentration, the surfactant ion activity remains nearly constant; under these conditions almost all surfactant molecules bind to HSA, $C_7F_{15}COO^-$ ions bind to specific sites on protein due to electrostatic interactions. A second transitional binding regime occurs when all the basic sites are occupied by a specifically bound surfactant, from $[S]_{total} = 12$–16 mM. Binding in this regime is evidently due to favorable hydrophobic interactions between fluorocarbons tails of surfactant molecules and hydrophobic proteins domains. We can see from the two different slopes of the emf vs. $[S]_{total}$ curve that in this regime surfactant binds to HSA in two steps. Finally, there is a new change in the slope of emf values vs. $[S]_{total}$ curve, at about $[S]_{total} > 16$ mM that determines the end of surfactant–HSA interactions and we assume that this effect on the emf is due only to surfactant molecule free.

The binding isotherm (Figure 2) can be obtained from data in Figure 1. Proper fitting of emf values findings gives ν values[28,29]. According to the fit in Figure 2, $C_7F_{15}COO^-Na^+$ manifests high affinity for HSA molecules.

Sodium perfluorooctanoate interacts more strongly with HSA than with other anionic surfactants,[30,31] avoiding precipitation of the protein at low or high surfactant concentrations. This can be explained by the presence of the fluorinated chains in the surfactant molecules. Perfluorinated chains combine two characteristics that are usually considered to be antinomic: they are extremely hydrophobic and hydrophilic at the same time. Therefore, surfactant molecules interact strongly so much with lipophobic as lipophilic residues of HSA domains.

The strong hydrophobic and low van der Waals (due to low polarizability of fluorine) interactions possessed by fluorinated chains dramatically increase the tendency of fluorinated amphiphiles to protein assemble in water. Saturation of all the binding sites correspond to about 6 g of surfactant per gram of the protein.

The binding data obtained can be presented in different ways, such as Klotz[32] and Scatchard[33] plots, and their interpretation can be carried out following schemes. One of the most popular concepts introduced recently is the binding capacity concept (Θ). It is the homotropic second derivative of the binding potential with respect to the chemical potential of the

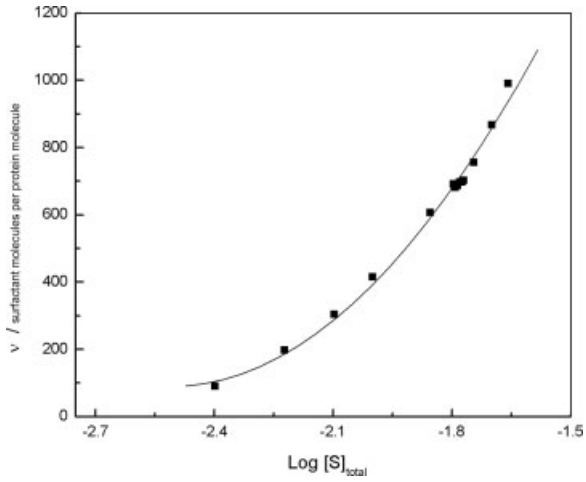

FIGURE 2 Binding isotherm for sodium perfluorooctanoate ($C_7F_{15}COO^-Na^+$) on the interaction with HSA at 25°C. The HSA concentration was 18 μM. The solid line was fitted as described in the text.

ligand (μ_i) and provides a measure of the steepness of the binding isotherm.[34] It represents the change in the number of moles of ligand per mole of macromolecule (ν) that accompanies a change in the chemical potential of that ligand.

By considering the ideal behavior ($\mu_i = \mu_i^0 + RT \ln[S]_{free}$), binding capacity is equal to

$$\Theta = \left(\frac{\partial \nu}{\partial \mu_i}\right) T,P,\mu_{j\neq i} = \left(\frac{1}{RT}\frac{\partial \nu}{\partial \ln[S]_{free}}\right) T,P,\mu_{j\neq i} \quad (1)$$

where R, T, and $[S]_{free}$ are gas constant, absolute temperature, and free concentration of the ligand, respectively.

For such a system, the binding data can be analyzed on the basis of empirical Hill equation[35]:

$$\nu = \frac{g(k_H[S]_{free})^{n_H}}{1 + (k_H[S]_{free})} \quad (2)$$

This can be written in the logarithmic form as follows:

$$\ln\left(\frac{\nu}{g-\nu}\right) = n_H + \ln k_H + n_H \ln[S]_{free} \quad (3)$$

where g, k_H, and n_H are the number of ligand-binding sites, Hill binding constant, and Hill coefficient, respectively.

Using Eq. (1), the binding capacity is equal to

$$\Theta = \frac{n_H \nu (g-\nu)}{gRT} \quad (4)$$

The Hill coefficient is defined as the slope of the Hill graph,

$$n_H = \frac{d\ln\left(\frac{y}{1-y}\right)}{d\ln[S]_{free}} = \frac{1}{y(1-y)}\frac{dy}{d\ln[S]_{free}} \quad (5)$$

where y is the fractional saturation of the macromolecule by the ligand, which is defined as follow:

$$y = \frac{\nu}{g} \quad (6)$$

From the definition of binding capacity [Eq. (1)], the following equation can be written:

$$n_H = \frac{RT\Theta}{gy(1-y)} \quad (7)$$

$$\Theta = \frac{n_H \nu (1-y)}{RT} \quad (8)$$

Equation (8) can be rearranged to the following form:

$$\frac{RT\Theta}{\nu} = n_H - \frac{n_H \nu}{g} \quad (9)$$

This equation suggests that the plot of $RT\Theta/\nu$ vs. ν for a system with g identical and dependent binding sites, should be linear. The slope and the y and x intercepts are equal to ($-n_H/g$), n_H and g, respectively.

Figure 3 shows the variation of $RT\Theta/\nu$ vs. ν for the binding of $C_7F_{15}COO^-Na^+$ to HSA. This curve can be divided to two linear regions, which implies that for HSA–$C_7F_{15}COO^-Na^+$ interactions all of the binding sites for such a system can be dividing into two categories, each of them related to a binding set. This is in complete accord with our previous analysis (Figure 1), which supposed the existence of two possible places of union.

The values of the x-intercept of the first and second part of the curve should be equal to g_1 and $g_1 + g_2$ respectively. The values of n_{H1} and n_{H2} can be determined from the slope of the fits.

The values of: 4.19 ± 0.02, 3.28 ± 0.03, 1414 ± 28, and 2565 ± 52 were estimated for n_{H1}, n_{H2}, g_1, and g_2, respectively.

Employing Eq. (3), we determined the Hill binding constants for such interactions. It was found that

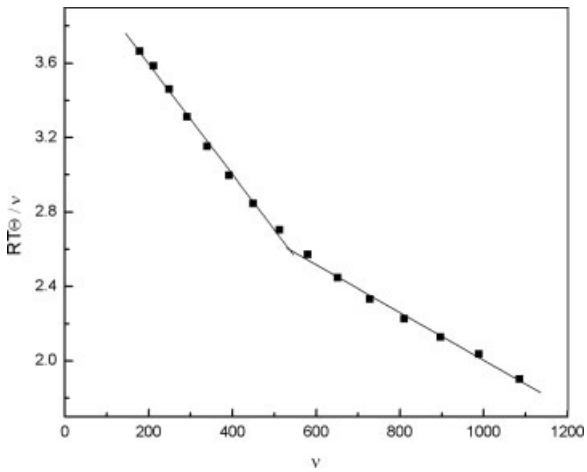

FIGURE 3 Variation of $RT\Theta/\nu$ vs. ν for the binding of $C_7F_{15}COO^-Na^+$ to HSA.

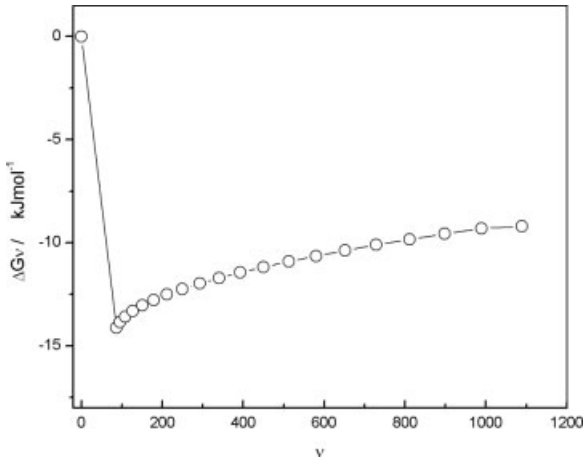

FIGURE 4 Gibbs energy of binding of $C_7F_{15}COO^-Na^+$ to HSA as a function of surfactant ions bound (ν) at 25°C.

$k_{H1} = 1.44 \times 10^5$ and $k_{H2} = 3.17 \times 10^4$. For all obtained values, the error was less than 5%.

To obtain the Gibbs energies per surfactant bound ($\Delta G\nu$) for the HSA– $C_7F_{15}COO^-Na^+$ interaction, the binding isotherm (Figure 2) was fitted to polynomials of the form:

$$\nu = a + b(\log[S]) + c(\log[S])^2 + \ldots \qquad (10)$$

where ν is the average number of surfactant molecules bound per monomeric HSA molecule and [*S*] the surfactant concentration. The order of the polynomial was chosen to give the highest correlation coefficient and lowest error over the data point range.

Polynomials were used to calculate the Wyman binding potentials (π) as a function of ν from the following equations[36]:

$$\pi = 2.303RT\left(\begin{matrix}(\log[S])_\nu \\ (\log[S])\nu(=0)\end{matrix}\ \nu\ d(\log[S])\right) \qquad (11)$$

$$\pi = 2.303.RT\{a(\log[S]) + b(\log[S])^2 + c(\log[S])^3 + \ldots\} \qquad (12)$$

The equilibrium constant (*K*) as a function of ν were calculated from the equation:

$$\pi = RT\ln(1 + K[S]^\nu) \qquad (13)$$

and hence $\Delta G\nu$ as a function of ν from

$$\Delta G_\nu = -\frac{RT\ln K}{\nu} \qquad (14)$$

This procedure leads to smooth curve of ΔG_ν vs. ν (Figure 4). $\Delta G_\nu \to 0$ at $\nu = 0$ so that plot shows a minimum corresponding to the most tightly bound ligands at low values of ν, then the curve tend to a limiting value, 9.2 kJ mol^{-1}. Similar curves were found in previous works for the interaction between surfactants and insulin.[37]

For a full description of proteins conformational changes upon ligand binding, we need to describe the movement of these transitions.

In the present work, we followed the kinetic of surfactant–HSA binding by ion selective electrodes measurements.

Figure 5 shows the variation of $[S]_{free}$ calculated from electrode selective measurements vs. time. The data evidence that there is a transition region where the $[S]_{free}$ changes steeply with time. We can observe that $[S]_{free}$ remains constant until a certain time value in which surfactant–protein binding begins. Then $[S]_{free}$ decreased to the extent that more and more surfactant bound to the protein. In the end, $[S]_{free}$ remains constant again when all the possible places for the HSA–$C_7F_{15}COO^-Na^+$ union were covered.

The kinetic effect is likely to come from the slow diffusion of molecules into the inner areas of the folded protein. Faucher and Goddard[38] showed that the uptake of SDS by keratinous substrates followed linear dependence on the square root of time, which is consistent with diffusion-limited process. In regard to the question of kinetic effect, the work by Griffith and Alexander[39] is noteworthy. Their results show that attaining equilibrium adsorption of SDS on wool at 35°C may take several weeks. The kinetic results reported by the above authors for hexadecyl sulfate show that the system exhibit several local "plateau values" which could be considered as pseudo-equilibria.

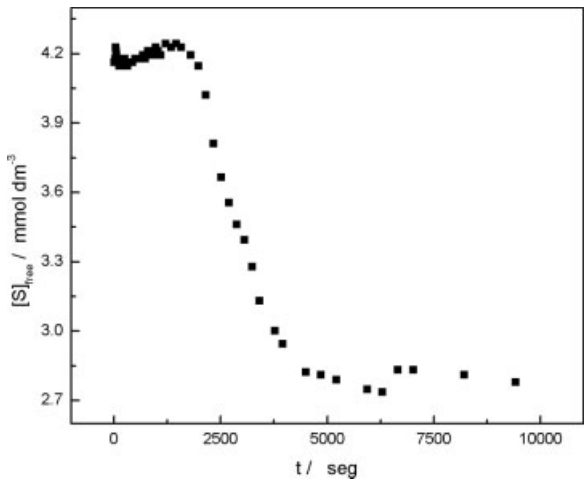

FIGURE 5 Kinetic absorption of $C_7F_{15}COO^-Na^+$ on HSA molecules. Calculated from electrode select measurements vs. time.

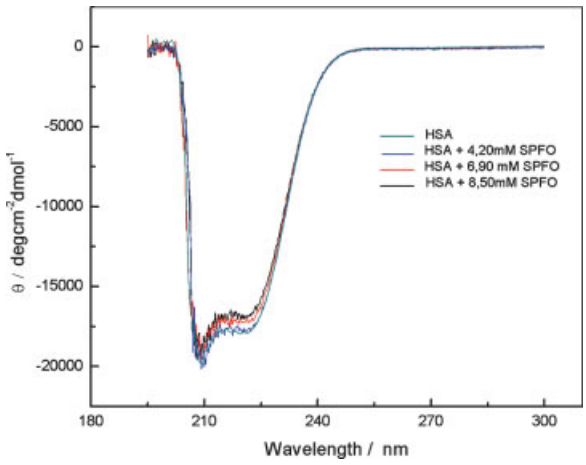

FIGURE 6 UV-CD spectrum of pure HSA and HSA–$C_7F_{15}COO^-Na^+$ dilute solutions Protein concentration was 8 μM.

A protein molecule is a macroscopic system; the disruption of this structure should be regarded as a change of the macroscopic state of the system. Information on the stability of a protein structure can be obtained only using temperature as variable, because temperature and energy of the system are the conjugate variables determining the state of a macroscopic system.[40] Thermal denaturation experiments were also performed and were used to validate our multistep unfolding model.

Figure 6 represents the typical UV-CD spectra for pure HSA and for HSA (8 μM) in the presence of $C_7F_{15}COO^-Na^+$ (4.20–8.50 mM). CD measurements provide information about secondary structure on proteins molecules and of how a polypeptide chain folds into different arrangements due to the binding of different ligands to these types of macromolecules.[41,42] It was observed that values of CD intensity for HSA in the presence of $C_7F_{15}COO^-Na^+$ are less negative. This behavior was attributable to HSA unfolding on account of its interaction with the surfactant molecules. The α-helical contents of free and combined HSA were calculated from $[\theta]\lambda$ value at $\lambda = 222$ nm using the following equation[43]:

$$\alpha\ (\%) = \left[\frac{-[\theta]_{222} - 4000}{33000 - 4000}\right] \times 100 \qquad (15)$$

where $[\theta]_{222}$ is the observed $[\theta]_\lambda$ at 222 nm, 4000 is the $[\theta]_\lambda$ of the β-form and random coil conformation at 222 nm, and 33,000 is the $[\theta]_\lambda$ value of a pure α-helix at 208 nm.

The calculated $\alpha(\%)$ varied from 53.1% for HSA pure to 49.8% for HSA in presence of surfactant (8.50 mM). We presume that due to surfactant interaction the HSA molecule in its native form (N) transitions to a unfolded form. We used UV-CD spectrophothometric measurements to study HSA thermal unfolding and conformational transitions induced by changes in temperature and concentration of C_7F_{15} COO^-Na^+ (Figure 7a and b).

From the plot $[\theta]_\lambda$ vs. T for native HSA, the data show that there is a transition region over which the $[\theta]_\lambda$ changes with temperature and shows two plateaus that correspond with two different conformational forms, (Figure 7a). Unfolding of HSA appeared to occur as a single step.

When surfactant is added, monitoring $[\theta]_\lambda$ at 222 nm variation with T for 4.20 mmol dm^{-3} and 5.50 mmol dm^{-3} surfactant concentration, we can obtain evidence of two unfolding steps, in qualitative agreement with the multistep unfolding during chemical denaturation[20] (Figure 7b). We can distinguish one first plateau and then a variation of $[\theta]_\lambda$ with T, but we cannot see the second plateau, which may indicate that the conforma-

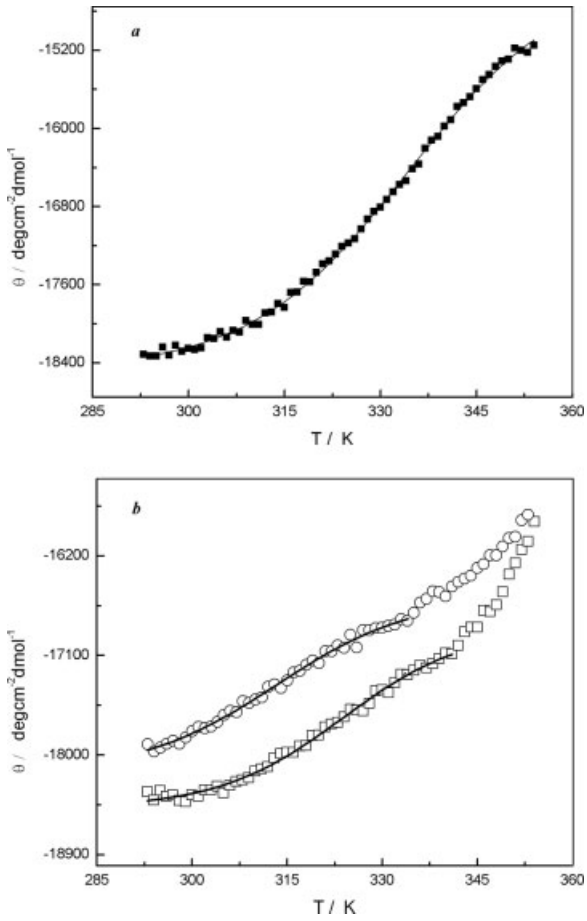

FIGURE 7 Thermal unfolding curve. (a) HSA pure. (b) HSA in presence of low surfactant concentration, (□) 4.20 mM of $C_7F_{15}COO^-Na^+$ and (○) 5.50 mM of $C_7F_{15}COO^-Na^+$.

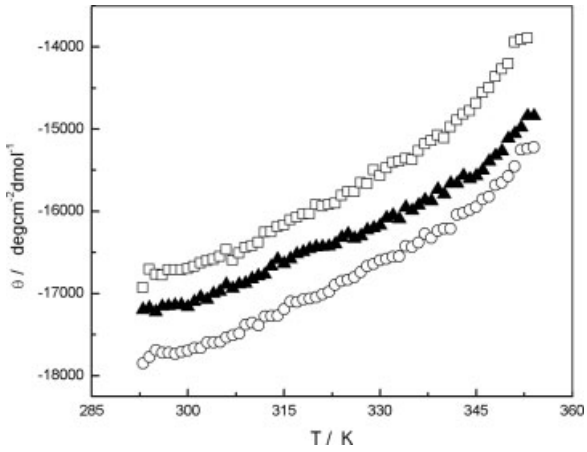

FIGURE 8 Thermal unfolding curve of HSA in the presence of high surfactant concentration. (○) 6.80 mM of $C_7F_{15}COO^-Na^+$, (▲) 6.90 mM of $C_7F_{15}COO^-Na^+$, and (□) 8.50 mM of $C_7F_{15}COO^-Na^+$.

tional transition is finished. We supposed that surfactant creates an additional stabilization against the action of the temperature that delays the unfolded process. This stabilization effect became greater as surfactant concentration increases. From 6.80 mmol dm^{-3} to 8.50 mmol dm^{-3} surfactant concentration we can not distinguish an intermediate form or the end of the conformational transition (Figure 8).

The thermal unfolded curves are analyzed in exactly the same way as in the chemical denaturant unfolding curves, but yields ΔG as a function of temperature rather can be used to determine the melting temperature (T_m), the entropy change at T_m (ΔS_m), the enthalpy change at T_m (ΔH_m) and the difference in heat capacity (ΔC_p) between the folded and unfolded conformations.

The thermal melting curve of HSA and HSA–$C_7F_{15}COO^-Na^+$ were examined using a modified form of the Gibbs–Helmholtz equation[44–46]:

$$\Delta G(T) = \Delta H\left(1 - \frac{T}{T_m}\right) - \Delta C_p\left[T_m - T + T\ln\left(\frac{T}{T_m}\right)\right] \quad (16)$$

where $\Delta G(T)$ is ΔG at a temperature T. Equation (16) was used to fit thermal unfolding parameters by using a nonlinear least-squares fit and successive iterations using the Marquardt–Levenberg routine. A minimum of 30 iterations or more was performed until the fractional change in the χ^2 value was within the tolerance limit (Figure 9).

The unfolding curve derived from measurements of HSA–$C_7F_{15}COO^-Na^+$ could not be fit to Eq. (16) when surfactant concentration was greater than 6.80 mmol · dm^{-3} because there was no postunfolding region, owing to the inability of our instrument to heat samples beyond 82°C.

Given that energy transfer is not possible under these experimental conditions, the spectroscopic changes provide evidence of a global change in protein structure due to surfactants molecules binding. These changes affect secondary protein structure—hence the structural changes involving domain separation must also have a direct effect on α-helix.

The found values of the thermal unfolding parameters for HSA native, $T_m = 68.9°C$, $\Delta H_m = 359.74$ kJ mol^{-1}, $\Delta C_p = 9.44$ kJ mol^{-1}, and $\Delta S_m = 1.05$ kJ mol^{-1} K^{-1} are of the same order as those found in literature.[47–50] When [$C_7F_{15}COO^-Na^+$] = 4.20 and

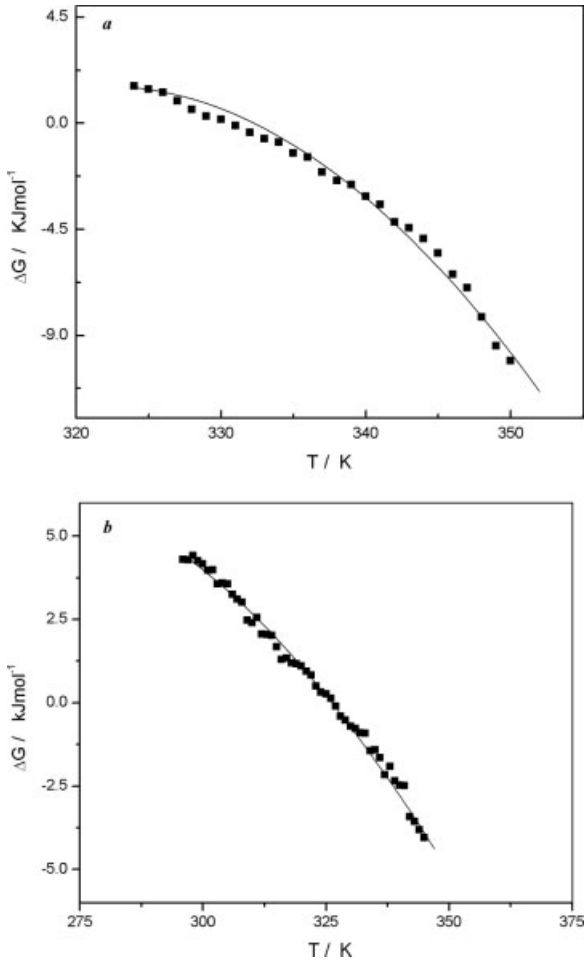

FIGURE 9 Gibbs energy of unfolding (ΔG) of HSA (8 μM) as a function of temperature. (a) HSA pure and (b) HSA in the presence of 5.50 mM of $C_7F_{15}COO^-Na^+$. The solid line represents a best fit of Eq. (16) used to determine the thermodynamics parameters of unfolding.

5.20 mmol dm^{-3}, the thermodynamic thermal unfolding data obtained for HSA–$C_7F_{15}COO^-Na^+$ intermediate forms were: T_m = 47.8 and 40.4°C; ΔH_m = 89.27 and 76.73 kJ mol^{-1} and ΔS_m = 0.28 and 0.25 kJ mol^{-1} K^{-1}, respectively. The value for $\Delta C_{p,}$ found for both intermediate forms, was approximately zero.

The small values of ΔS_m indicated that the intermediate conformational transition step was not entropically controlled, and that is independent of the surfactant concentration. Furthermore, this intermediate form, compared with HSA native form, shows practically not heat capacity variation.

CONCLUSION

We have studied the interaction between sodium perfluorooctanoate and HSA in aqueous solution.

We have used an ion-selective electrode to determine the amount of surfactant bound to HSA. The interaction between HSA and $C_7F_{15}COO^-Na^+$ were inferred from the change in slope of the emf curve.

According to emf findings, the interaction between HSA and the surfactant molecules results in a true conformational change on protein molecules. As we can see from the two different slopes of emf vs. $[S]_{total}$ curve, surfactant binds to HSA in two steps.

Sodium perfluorooctanoate interacts much more strongly with HSA than other anionic surfactants and does not cause precipitation of the protein at low or high surfactant concentration. The average number of surfactant molecules absorbed per protein molecule (at 28 m*M* of surfactant concentration) was found to be ≈900, about 6 g of surfactant per gram of protein.

We have represented the binding data obtained such as Klotz and Scatchard plots to obtain g, k_H, and n_H values.

Variation of $RT\Theta/\nu$ vs. ν showed two linear regions. This fact implies that for such system interactions can be divided into two categories. The values of 4.19 ± 0.02, 3.28 ± 0.03, 1414 ± 28, and 2565 ± 52 were estimated for n_{H1}, n_{H2}, g_1, and g_2, respectively. It was found that $k_{H1} = 1.44 \times 10^5$ and $k_{H2} = 3.17 \times 10^4$.

Fitting the binding isotherm to a polynomial form, we can calculate the Wyman binding potential (π) and obtain the Gibbs energies per surfactant bound (ΔG_ν). This procedure leads to smooth curve of ΔG_ν vs. ν, $\Delta G_\nu \to 0$ at $\nu = 0$ so that plot shows a minimal corresponding to the most tightly bound ligands at low values of ν, then the curve tend to a limiting value (9.2 kJ mol^{-1}).

For a full description of proteins conformational changes upon ligand binding, we have studied the movement of these transitions and the thermal denaturation effect.The kinetic effect shows a slow diffusion of molecules into the inner areas of the folded protein.

Thermal denaturation effect was followed through UV-CD measurements and used to validate our multistep unfolding model. It was observed that values of CD intensity for HSA in aqueous solution are less negative in presence of $C_7F_{15}COO^-Na^+$. The calculated α (%) varied from 53.1% for HSA pure to 49.8% for HSA in presence of surfactant (8.50 m*M*). This fact was due to HSA unfolding on account of its interaction with the surfactant molecules.

Temperature unfolding curves showed a multistep unfolding for low (4.20–5.50 m*M*) surfactant concentration. We can distinguish an intermediary step in unfolding transition, but we were not capable to see the end of conformational transition. We supposed that surfactant creates an additional stabilization effect against the action of temperature that delays the unfolding process. This stabilization effect became greater as surfactant concentration increases. From 6.80 to 8.50 m*M* surfactant concentration, we cannot identify an intermediate form or the end of transition, owing to the inability of our instrument to heat samples beyond 82°C.

Given that energy transfer is not possible under these experimental conditions, the spectroscopic changes provide evidence of a global change in protein structure due to surfactants molecules binding. These change affect secondary protein structure—hence the structural changes involving domain separation must also have a direct effect on α-helix.

This research was funded by the Spanish Ministry of Science and Technology (Project MAT2002-00608), by the European Regional Development Fund (ERDF) and by Xunta de Galicia (Project PGIDIT03PXI20615PN). PVM thanks Fundación Antorchas, Argentina (14308/110), and Banco Rio for financial support to travel to the University of Santiago de Compostela and participate in this research. PCS thanks the Consejo Nacional de Investigaciones Científicas y Técnicas de la República Argentina (CONICET) for the PIP#2739, which enabled him to travel to the University of Santiago de Compostela and work on this project. We thank Dr. José L. Mascareñas, from Organic Chemistry Department, Faculty of Chemistry, University of Santiago de Compostela, Spain, for permission for us to carry out the CD experiments in his laboratory.

REFERENCES

1. Krafft, M. P.; Riess J. G. Biochimie 1998, 80, 489–514.
2. Riess, J. G. In Fascinated by Fluorine; Banks, R. E., Ed.; Elsevier: Amsterdam, 2000.
3. Riess, J. G.; Krafft M. P. Mat Res Soc Bull 1999, 24, 42–48.

4. Chabert, P.; Foulletier, L.; Lantz, A. Procédé de preparation de liquides à application biologique et transporteurs d'oxygène 1975, Chabert, P.; Foulletier, L.; Lantz, A. Fr. Pat. 2, 452, 513.
5. Mathis, G.; Leempoel, P.; Ravey, J. C.; Selve, C.; Delpuech, J. J. J Am Chem Soc 1984, 106, 6162–6171.
6. Mukerjee, P.; Mysels, K. J. In Colloidal Dispersions and Micellar Behavior; Mittal, K. L, Ed.; ACS Symposium Series 9; American Chemical Society: Washington, DC, 1975.
7. Kunieda, H.; Shinoda, K. J Phys Chem 1976, 80, 2468–2470.
8. Robert, A.; Tondre, C. J Colloid Interf Sci 1984, 98, 515–522.
9. Ravey, J. C.; Stebe, M. J. Progr Colloid Polym Sci 1987, 73, 127–133.
10. Lattes, A.; Rico-Lattes, I. Art Cells Blood Subst Immob Biotech 1994, 22, 1007–1018.
11. Sticht, H.; Willbold, D.; Ejchart, A.; Rosin-Arbesfeld, F.; Yaniv, A.; Gazit, A.; Rosch, P. Eur J Biochem 1994, 225, 855–1861.
12. Jones, M. N. In Biochemical Thermodynamics, 1st ed.; Jones, M. N., Ed.; Elsevier: Amsterdam, 1985.
13. Jones, M. N.; Brass, A. In Food Polymers, Gels and Colloids; Dickinson, E., Ed.; Royal Society of Chemistry: London, 1991.
14. Berde, C. B.; Hudson, B. S.; Simoni, R. D.; Sklar, L. A. J Biol Chem 1979, 254, 391–400.
15. Peters, T. Adv Protein Chem 1985, 37, 161–245.
16. Sjoholm, I.; Ekman, B.; Kober, A.; Ljungstedt-Pahlman, I.; Seiving, B.; Sjodin, T. Mol Pharmacol 1979, 16, 767–777.
17. Kragh-Hansen, U. Mol Pharmacol 1988, 34, 160–171.
18. Nerli, B.; Romanini, D.; Picó, G. Chem Biol Interacts 1977, 104, 179–202.
19. Messina, P.; Prieto, G.; Dodero, V.; Cabrerizo-Vílchez, M. A.; Maldonado-Valderrama, J.; Ruso, J. M.; Sarmiento, F. Langmuir 2005, submitted.
20. Messina, P.; Prieto, G.; Ruso, J. M.; Sarmiento, F. J Phys Chem B 2005, accepted.
21. Dockal, M.; Carter, D. C.; Rüker, F. J Biol Chem 2000, 275, 3042–3050.
22. Goddard, E. D. Colloids Surf 1986, 19, 255–300.
23. Goddard, E. D. Colloids Surf 1986, 19, 301–329.
24. Steinhardt, J.; Reynolds, J. A. Multiple Equilibria in Proteins: Academic Press: New York, 1969.
25. Tanford, C. The Hydrophobic Effect: Formation of Micelles and Biological Membranes, 2nd ed.; Wiley—Interscience: New York, 1980.
26. Schwuger, M. J.; Bartnik, F. G. In Anionic Surfactants; Ed.; Marcel Dekker Surfactants Sci. Series; Marcel Dekker: New York, 1980; Vol 10.
27. Takisawa, N.; Brown, P.; Bloor, D. M.; Hall, D. G.; Wyn-Jones, E. J Chem Soc Faraday Trans 1989, 85, 2099–2112.
28. Liu, J.; Nakama, M.; Takisawa, N.; Shirahama, K. Colloids Surf A 1999, 150, 275–281.
29. Shirahama, K.; Liu, J.; Aoyama, I.; Takisawa, N. Colloids Surf A 1999, 147, 133–138.
30. Sun, M. L.; Tillon, R. D. Colloids Surf B 2001, 20, 281–293.
31. Gelamo, E. L.; Silva, C. H. T. P.; Imasato, H.; Tabak, M. Biochim Biophys Acta 2002, 1594, 84–99.
32. Klotz, I. M.; Huston, D. L. J Biol Chem 1975, 250, 3001–3009.
33. Scatchard, G. Ann NY Acad Sci 1949, 51, 660–672.
34. Cera, E.; Gill, S.; Wyman, J. Proc Natl Acad Sci USA 1988, 85, 449–452.
35. Hill, A.V. J Biochem 1913, 7, 471–480.
36. Wyman, J. J Mol Biol 1965, 11, 631–644.
37. Sarmiento, F.; Prieto, G.; Jones, M. N. J Chem Soc Faraday Trans 1992, 88, 1003–1007.
38. Faucher, J. A.; Goddard, E. D. J Soc Cosmet Chem 1978, 29, 323–337.
39. Griffith, J. C.; Alexander, A. E. J Colloids Interface Sci 1967, 25, 311–316, 317–321.
40. Privalov, P. L. Annu Rev Biophys Biophys Chem 1989, 18, 47–69.
41. Woody, R. W. Methods Enzymol 1995, 246, 34–71.
42. Schmid, F. X. In Protein Structure: A Practical Approach; Creighton, T. E., Ed.; IRL Press: Oxford, 1989.
43. Lu, Z. X.; Cui, T.; Shi, Q. L. Applications of Circular Dischroism and Optical Rotatory Dispersion in Molecular Biology, 1st ed.; Science Press, 1987.
44. Pace, C. N.; Laurents, D. V. Biochemistry 1989, 28, 2520–2525.
45. Pace, C. N. Trends Biotechnol 1990, 8, 93–98.
46. Kaushik, J. N.; Bhat, R. J Phys Chem B 1998, 102, 7058–7066.
47. Flora, K.; Brennan, J. D.; Baker, G. A.; Doody, M. A.; Bright, F. V. Biophys J 1998, 75, 1084–1096.
48. Picó, G. A. Biochem Mol Biol Int 1995, 36, 1017–1023.
49. Picá, G. A. Biochem Mol Biol Int 1996, 38, 1–6.
50. Picó, G. A. Int J Biol Macromol 1997, 20, 63–73.

Reviewing Editor: Laurence A. Nafie